

Characterization of the Ni(III) Intermediate in the Reaction of (1,4,8,11-Tetraazacyclotetradecane)nickel(II) Perchlorate with KHSO_5 : Implications to the Mechanism of Oxidative DNA Modification

Jeffrey N. Stuart, Adrienne L. Goerges, and Jeffrey M. Zaleski*

Department of Chemistry, Indiana University, Bloomington, Indiana 47405

Received May 26, 2000

We report the detection and characterization of the Ni(III) intermediates generated by reaction of (1,4,8,11-tetraazacyclotetradecane)nickel(II) perchlorate with KHSO_5 . Four Ni(III) intermediates can be trapped or detected through variation in Cl^- or KHSO_5 concentrations. Upon oxidation of $[\text{Ni}(\text{cyclam})]^{2+}$ by 2.5 equiv of KHSO_5 , deprotonation of the cyclam ligand generates two red Ni(III) species with $\lambda_{\text{max}} = 530 \text{ nm}$ and $g_{\perp} = 2.20$ and $g_{\parallel} = 2.02$ or $g_{\perp} = 2.16$ and $g_{\parallel} = 2.01$ for the axial 4-coordinate or 6-coordinate dichloride species, respectively. These forms decay to Ni(II) products via complex ligand oxidation mechanisms. The Ni(III) dichloride species can be reprotonated and subsequently binds to DNA via an outer-sphere interaction as evidenced by the inverted sign of the CD signal near 400 nm. Cumulatively, the results indicate that the Ni(III) center is coordinately saturated under excess chloride conditions but is still able to interact with DNA substrates. This suggests alternative mechanistic pathways for DNA modification by reaction of $[\text{Ni}(\text{cyclam})]^{2+}$ with KHSO_5 and possibly other Ni(II) complexes as well.

Introduction

Concerns over environmental human exposure to sulfite (SO_3^{2-}) due to its potential role in mutagenesis and carcinogenesis^{1,2} have led to increased interest in understanding the biological chemistry of this species. Sulfite can be generated by the autoxidation of SO_2 , which is a component of industrial emissions^{1,3,4} and food preservatives.^{1,5} It is now established that metal ions can catalyze the autoxidation of sulfur oxides,^{4,6–12} which leads to the production of sulfite and the higher oxidized form monoperoxysulfate (HSO_5^-). These species are thought to ultimately form sulfur oxy radicals ($\text{SO}_x^{\bullet-}$, $x = 3–5$) which are toxic to biological materials.^{1,3,4} The possibility that in vivo metal ions such as those in metalloproteins, or adventitious metal–protein/DNA complexes could catalyze the production of $\text{SO}_x^{\bullet-}$ radicals leads to important questions regarding the mechanism of formation and the specific biological damage caused by these species.

To this end, both peptide and macrocyclic nitrogen-based ligands form $[\text{NiN}_4]^{2+}$ complexes with Ni(II) and have been shown to react with oxidants (e.g., KHSO_5) to form reactive intermediates that induce protein–protein cross-linking^{13,14} and, in the presence of various DNA structural motifs, DNA modi-

fication.^{15,16} The reactivity of these systems with DNA is not general, but rather dependent upon the nature of the ligands to Ni(II), as well as the oxidant concentration and ionic strength conditions under which the reactions are performed. Under conditions of equimolar KHSO_5 and low ionic strength, Ni(II)·Xaa-Xaa-His metalloproteins yield C4' H-atom abstraction products derived from minor groove DNA binding.^{16,17} In contrast, excess KHSO_5 and high ionic strength conditions lead to solvent exposed guanine oxidation,^{17,18} which is proposed to derive from a nickel-bound sulfate radical species that is not tightly associated with the narrow minor groove of DNA, but rather coordinated directly to the N7 position of guanine.¹⁹ Under these latter conditions, the oxidative reactivity of macrocyclic Ni(II) reagents with solvent-exposed guanines such as those found in bulges, mismatches, and hairpin loops²⁰ has prompted their use as tertiary structure probes of complex RNA conformations.²¹

It has been suggested that formation of $\text{SO}_4^{\bullet-}$ is likely a key species responsible for the oxidation of guanine by KHSO_5 .¹⁸ The proposed mechanism¹⁵ involves direct oxidation of $[\text{NiN}_4]^{2+}$ by HSO_5^- , to form $\text{SO}_5^{\bullet-}$ and OH^- , as well as a transient $[\text{NiN}_4]^{3+}$ species in which the metal center is formally Ni(III) (eq 1). The 3+ charge and d^7 electronic configuration of the

* Author to whom correspondence should be addressed (E-mail: zaleski@indiana.edu).

- (1) Shapiro, R. *Mutat. Res.* **1977**, *39*, 149.
- (2) Reed, G. A.; Curtis, J. F.; Mottley, C.; Eling, T. E.; Mason, R. P. *Proc. Natl. Acad. Sci. U.S.A.* **1986**, *83*, 7499.
- (3) Neta, P.; Huie, R. E. *Environ. Health Perspect.* **1985**, *64*, 209.
- (4) Brandt, C.; Eldik, R. v. *Chem. Rev.* **1995**, *95*, 5.
- (5) Hyatsu, H. *Prog. Nucleic Acid Res. Mol. Biol.* **1976**, *16*, 75.
- (6) Coichev, N.; Eldik, R. v. *Inorg. Chem.* **1991**, *30*, 2375.
- (7) Fronaeus, S.; Berglund, J.; Elding, L. I. *Inorg. Chem.* **1998**, *37*, 4939.
- (8) Berglund, J.; Fronaeus, S.; Elding, L. I. *Inorg. Chem.* **1993**, *32*, 4527.
- (9) Bhattacharya, S.; Ali, M.; Gangopadhyay, S.; Banerjee, P. *J. Chem. Soc., Dalton Trans.* **1994**, 3733.
- (10) Shi, X. *J. Inorg. Biochem.* **1994**, *56*, 155.
- (11) Connick, R. E.; Zhang, Y. X. *Inorg. Chem.* **1996**, *35*, 4613.
- (12) Muller, J. G.; Burrows, C. J. *Inorg. Chim. Acta* **1998**, *275–276*, 314.

- (13) Brown, K. C.; Zhonghua, Y.; Burlingame, A. L.; Craik, C. S. *Biochemistry* **1998**, *37*, 4397.
- (14) Brown, K. C.; Yang, S.-H.; Kodadek, T. *Biochemistry* **1995**, *34*, 4733.
- (15) Burrows, C. J.; Muller, J. G. *Chem. Rev.* **1998**, *98*, 1109.
- (16) Long, E. C. *Acc. Chem. Res.* **1999**, *32*, 827.
- (17) Liang, Q.; Ananias, D. C.; Long, E. C. *J. Am. Chem. Soc.* **1998**, *120*, 248.
- (18) Muller, J. G.; Hickerson, R. P.; Perez, R. J.; Burrows, C. J. *J. Am. Chem. Soc.* **1997**, *119*, 1501.
- (19) Shih, H.; Tang, N.; Burrows, C. J.; Rokita, S. E. *J. Am. Chem. Soc.* **1998**, *120*, 3284.
- (20) Chen, X.; Burrows, C. J.; Rokita, S. E. *J. Am. Chem. Soc.* **1992**, *114*, 322.
- (21) Chen, X.; Woodson, S. A.; Burrows, C. J.; Rokita, S. E. *Biochemistry* **1993**, *32*, 7610.



Ni(III) center makes it prone to form 6-coordinate tetragonal structures. In the presence of DNA, N7 of guanine is therefore a logical candidate to contribute to the inner-sphere coordination at the Ni(III) center.^{22–24} Inner-sphere coordination by guanine is proposed to derive from the conversion of poly(dG-dC) from B to Z helical form by monitoring the ellipticity of the nucleotide at 295 nm in the presence and absence of Ni(III).²⁵ Additionally, Ni–N7 coordination is inferred from paramagnetic effects upon ¹H NMR spectra of 5'-GMP and select DNA oligonucleotides in the presence of certain nickel complexes.^{19,26} These data, coupled with guanine-specific oxidation and the fact that radicals such as $\text{SO}_4^{\bullet-}$ or OH^\bullet are not detected free in solution,¹⁸ have led to a proposed structure for the intermediate that contains either a Ni(III) center with N7 of guanine and $\text{SO}_4^{\bullet-}$ bound axially or the isoelectronic N7–Ni(IV)– SO_4^{2-} species. Although it is clear that the available experimental results are consistent with the proposed mechanism, a sufficient number of questions persist regarding the chemical pathway for oxidation of Ni(II) complexes by KHSO_5 and the implications of individual steps to DNA oxidation.

Within this theme, we report the characterization of the in situ Ni(III) intermediate generated by oxidation of $[\text{Ni}(\text{cyclam})]^{2+}$ (**1**) by KHSO_5 in both the absence and presence of a 17-base oligonucleotide containing a guanine-rich hairpin loop (Scheme 1). We have monitored this reaction by electronic absorption and freeze–quench EPR spectroscopies as a function of Cl^- concentration which is in large excess in experiments exhibiting guanine oxidation products.^{16,20,23} Our results demonstrate that, within the first 30 s of the reaction, a 6-coordinate, axial Ni(III) species is formed which subsequently decays to EPR silent Ni(II) products. From the *g*-values and corresponding superhyperfine coupling, we propose a structure for the Ni(III) center immediately following oxidation and discuss the implications of this species to current mechanistic proposals for the overall oxidative modification of DNA by these agents.

Experimental Section

Materials. All chemicals were of the highest purity available from Aldrich and Sigma Chemical Companies and used as received. The desalted oligonucleotide, d(AGTCTATGGGTTAGACT), was purchased from Genosys Laboratories and used without further purification. The complexes (1,4,8,11-tetraazacyclotetradecane)nickel(II) perchlorate ($[\text{Ni}(\text{cyclam})](\text{ClO}_4)_2$, **1**)²⁷ and (1,4,8,11-tetraazacyclotetradecane)nickel(III) (SO_4)(ClO_4) ($[\text{Ni}(\text{cyclam})](\text{SO}_4)(\text{ClO}_4)$, **2**)²⁸ were synthesized and characterized according to established literature procedures.^{29,30} Compound purity was confirmed by ¹H NMR (for Ni(II)), IR, and elemental analysis.

(22) Muller, J. G.; Zheng, P.; Rokita, S. E.; Burrows, C. J. *J. Am. Chem. Soc.* **1996**, *118*, 2320.

(23) Muller, J. G.; Chen, X.; Dadiz, A. C.; Rokita, S. E.; Burrows, C. J. *J. Am. Chem. Soc.* **1992**, *114*, 6407.

(24) Burrows, C. J.; Rokita, S. E. *Acc. Chem. Res.* **1994**, *27*, 295.

(25) Burrows, C. J.; Muller, J. G.; Shih, H.; Rokita, S. E. *Supramol. Stereochem.* **1995**, *57*.

(26) Shih, H.-C.; Kassahun, H.; Burrows, C. J.; Rokita, S. E. *Biochemistry* **1999**, *38*, 15034.

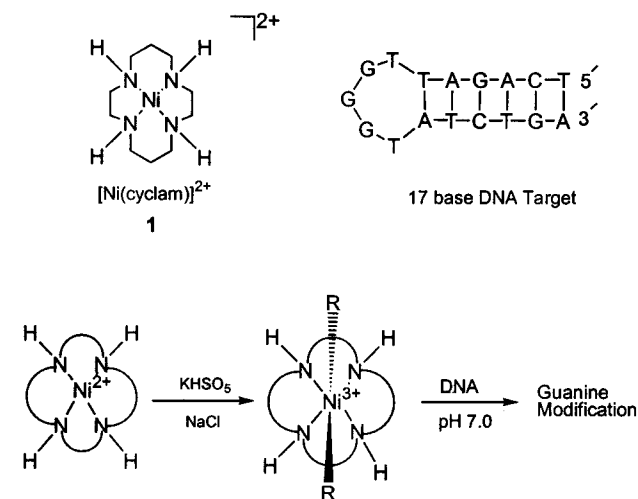
(27) Bosnich, B.; Tobe, M. L.; Webb, G. A. *Inorg. Chem.* **1965**, *4*, 1109. **CAUTION!** Perchlorate salts are potentially explosive, and great care should be taken when working with these materials (cf.: *J. Chem. Educ.* **1973**, *50*, A335; *Chem. Eng. News* **1983**, *61*, 1 (Dec. 5), 4; **1963**, *41* (July 8), 47).

(28) Gore, E. S.; Busch, D. H. *Inorg. Chem.* **1973**, *12*, 1.

(29) Barefield, E. K.; Wagner, F.; Herlinger, A. W.; Dahl, A. R. (1,4,8,11-Tetraazacyclotetradecane)Nickel(II) Perchlorate and 1,4,8,11-tetraazacyclotetradecane. In *Inorganic Syntheses*; Basolo, F., Ed.; McGraw Hill Book Co.: New York, 1976; Vol. XVI, p 220.

(30) Connolly, P. J.; Billo, E. J. *Inorg. Chem.* **1987**, *26*, 3224.

Scheme 1. General Reaction Scheme for the Oxidation of $[\text{Ni}(\text{cyclam})]^{2+}$ by KHSO_5 in the Presence of a 17-Base DNA Target



Physical Measurements. Proton NMR spectra were obtained on a Gemini 2000, 300 MHz spectrometer and referenced to phosphate buffer in D_2O at pD 7.0. Infrared spectra (Nujol and KBr) were obtained on a Nicolet 510P spectrometer. All electron paramagnetic resonance spectra were recorded at X-band (9.5 GHz) on an ESP 300 Bruker instrument using a liquid nitrogen finger dewar. Typical EPR conditions: microwave power, 10 mW; modulation amplitude, 5–20 G; modulation frequency, 100 kHz; receiver gain, 2×10^4 . The amount of Ni(III) generated upon oxidation of **1** was quantitated using a 1.0 or 3.0 mM standard sample of **2** in either a saturated aqueous sucrose or a 50:50 glycerol/water solution. EPR spectra were simulated using a Monte Carlo method,^{31,32} and all spin quantitations were performed within WinEPR Simfonia (Bruker Analytical Instruments). For all quantitations, the dependence of the signal intensity on microwave power was examined to avoid signal saturation conditions. Electronic spectra were taken on a Hewlett-Packard 8452A diode array UV/vis spectrometer and a Perkin-Elmer Lambda 19 UV/vis/near-IR spectrometer. Circular dichroism (CD) spectra were obtained on a Jasco J-715 spectropolarimeter equipped with ultraviolet and near-infrared photomultiplier tubes. For near-infrared electronic absorption and CD spectra, D_2O was used as the solvent to minimize spectral interference.

Oxidation of **1 with KHSO_5 .** All DNA solutions were prepared by dissolving the 17-base oligonucleotide in a phosphate-buffered (≥ 10 mM) saline (NaCl) medium (10:1 Cl^- :buffer) adjusted to pH 7.0. For Cl^- dependence studies (100 mM, 400 mM, and 1 M), the Cl^- :buffer ratio was maintained in order to keep the competition for solution anions constant during formation of the Ni(III) intermediate. To 190 μL of this solution were added sequentially 5 μL of a concentrated solution of **1** and 5 μL of a concentrated aqueous KHSO_5 solution, the latter to initiate the oxidation reaction. The final concentrations of **1** and DNA oligonucleotide were 1 mM, with KHSO_5 in 2.5-fold excess. Samples for spectroscopic measurements in the absence of DNA contained **1** at either 1 or 3 mM and KHSO_5 in 2.5-fold excess.

Results and Discussion

Spectroscopic Characterization of **2.** In order to determine the nature of the intermediate generated via oxidation of **1** by KHSO_5 in the presence and absence of DNA, we chose to first characterize the spectroscopic signatures of the Ni(III) center of **2** under our experimental conditions. Figure 1a shows an X-band EPR spectrum and simulation of **2** in a saturated aqueous sucrose matrix at 77 K. The spectrum exhibits a low-spin, axial

(31) Neese, F. *QCPE* **1995**, Bull. 15, 5.

(32) Gaffney, B. J.; Silverstone, H. J. *Biological Magnetic Resonance. In NMR of Paramagnetic Molecules*; Reuben, J., Berliner, J., Eds.; Plenum Press: New York, 1993; Vol. 13, p 1.

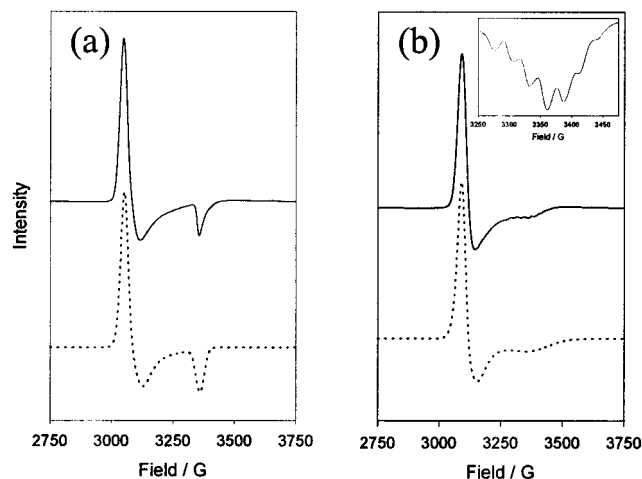


Figure 1. Observed (—) and calculated (···) X-band EPR spectra of **2** (3 mM) in a (a) saturated aqueous sucrose solution and (b) 100 mM phosphate buffer (pH 7.0) with 1 M Cl⁻ at 77 K. The g_{\parallel} region is expanded in panel b (inset) to illustrate the 7-line superhyperfine splitting pattern arising from two Cl⁻ bound axially ($A_{\text{Cl}} = 28$ G). Simulated EPR parameters: (a) $g_{\perp} = 2.20$; $g_{\parallel} = 2.02$; (b) $g_{\perp} = 2.16$; $g_{\parallel} = 2.01$.

signal ($g_{\perp} > g_{\parallel}$) with $g_{\perp} = 2.20$ and $g_{\parallel} = 2.02$ characteristic of a weakly distorted, tetragonally elongated center.^{33,34} The modest anisotropy of the g value relative to other Ni(III) species indicates that the center has two axially coordinating ligands in solution, likely from solvent or counterion. Additionally, no superhyperfine coupling to the four equatorial nitrogens ($I = 1$) is observed since the unpaired electron in this geometry resides in the d_{z^2} orbital of the Ni(III) and therefore interacts preferentially with the axial ligands.^{34,35} The EPR spectrum of **2** in phosphate buffer, pH 7.0 in the presence of excess Cl⁻ (Figure 1b) is very comparable, once again indicating a weak axial geometry at the Ni(III) center with $g_{\perp} = 2.16$ and $g_{\parallel} = 2.01$. The similarity of the g values suggests that an analogous structure is present in solution with two ligands occupying the axial positions. The superhyperfine splitting of g_{\parallel} into a 7-line pattern (Figure 1b, inset) indicates that these ligands are Cl⁻ ions ($I = 3/2$, $2nI + 1 = 7$, second derivative analysis: 1:2:3:4:3:2:1) under high salt conditions that couple strongly to the electron in the d_{z^2} orbital ($A_{\text{Cl}} = 28$ G).^{34,36,37} This is consistent with the X-ray crystal structure for [Ni(cyclam)Cl₂]⁺ which reveals coordinated Cl⁻ counterions occupying axial positions,³⁸ as well as the previously reported EPR spectrum of [Ni(cyclam)Cl₂]⁺.^{36,37}

In addition to the EPR signatures of the Ni(III) center, electronic absorption spectroscopy offers a distinct spectral profile indicative of the trivalent oxidation state of the Ni center via analysis of the ligand field transitions. In the region 5500–18000 cm⁻¹, one broad spectral feature is observed at ~13000 cm⁻¹ that can be fit using a combination of six Gaussian absorption profiles (Figure 2, Table 1). Since there are only a

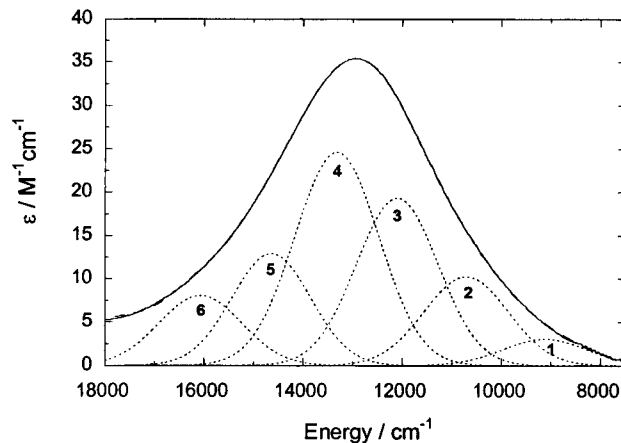


Figure 2. Ligand field region electronic absorption spectrum of **2** (3 mM) in 100 mM phosphate buffer (pH 7.0) with 1 M Cl⁻ at 298 K. The experimental spectrum (—) can be fit by six Gaussian band shapes (···) centered at 9124, 10711, 12105, 13323, 14645, and 16793 cm⁻¹, and is plotted against the resultant sum (---) of these components.

Table 1. Band Assignments for the Gaussian Resolved Electronic Absorption Spectrum of **2** in 100 mM Phosphate Buffer (pH 7.0) and 1 M Cl⁻

band	energy/cm ⁻¹	fwhm/cm ⁻¹	transition
1	9124	1998	² A _{1g} → ⁴ A _{2g}
2	10711	2000	² A _{1g} → ² E _g
3	12105	1940	² A _{1g} → ² E _g
4	13323	1998	² A _{1g} → ² B _{2g}
5	14645	1872	² A _{1g} → ⁴ E _g
6	16793	1965	² A _{1g} → ⁴ E _g

modest number of spectroscopic studies of Ni(III) species, and often ligand field bands are obscured by low-energy charge transfer transitions, tentative assignments of the features in Figure 2 can be made to a first approximation from spectral assignments of isoelectronic, low-spin Co(II) in local D_{4h} symmetry.^{39–41} From analysis of the EPR spectra in Figure 1, the Ni(III) center is 6-coordinate with two Cl⁻ ions coordinated axially resulting in a weak, tetragonally distorted center with the unpaired electron in the d_{z^2} orbital (Figure 3a). The magnitude of this distortion governs the relative energies of each of the d orbitals and thus the ligand field transition energies. It is clear from Figure 2 that several transitions must comprise the broad absorption envelope (fwhm = 4300 cm⁻¹) centered at ~13000 cm⁻¹. Based on the relatively small g value anisotropy of **2** in the presence of Cl⁻, the splitting of the ground state ²E_g term and the higher lying ⁴T_{1g} and ²T_{2g} states in weak tetragonal symmetry will result in seven transitions, six of which are close in energy.⁴⁰ The lowest energy transition will be that between the split components of the ground state ²E_g term, ²A_{1g} → ²B_{1g} in the local D_{4h} symmetry ($d_{z^2} \rightarrow d_{x^2-y^2}$), but it lies beyond our spectral limits of detection (<5500 cm⁻¹). To higher energy, we find six transitions that comprise the absorption envelope centered at ~13000 cm⁻¹. Assignment of these features is complicated by the fact that at weak to intermediate degrees of axial distortion, the splitting of the ²T_{2g} term in O_h symmetry generates ²B_{2g} and ²E_g states that are nearly isoenergetic with the spin-forbidden transitions of the ⁴T_{1g} state (⁴A_{2g} and ⁴E_g). Out-of-state spin-orbit coupling via the O' (and D₄') double group mixes orbital angular momentum into the ground state, which lends intensity to the spin-forbidden transitions. Subse-

(33) Jacobs, S. A.; Margerum, D. W. *Inorg. Chem.* **1984**, *23*, 1195.

(34) Margerum, D. W.; Anliker, S. L. *Nickel(III) Chemistry and Properties of the Peptide Complexes of Ni(II) and Ni(III)*. In *The Bioinorganic Chemistry of Nickel*; Lancaster, J. R., Jr., Ed.; VCH Publishers: New York, 1988; p 29.

(35) Sugiura, Y.; Mino, Y. *Inorg. Chem.* **1979**, *18*, 1336.

(36) Desideri, A.; Raynor, B.; Poon, C.-K. *J. Chem. Soc., Dalton Trans.* **1977**, 2051.

(37) Lappin, A. G.; McAuley, A. *The Redox Chemistry of Nickel*. In *Advances in Inorganic Chemistry*; Sykes, G., Ed.; Academic Press: Orlando, 1988; Vol. 32, p 241.

(38) Ito, T.; Sugimoto, M.; Toriumi, K.; Ito, H. *Chem. Lett.* **1981**, 1477.

(39) Lever, A. B. P. *Inorganic Electronic Spectroscopy*, 2nd ed.; Elsevier: Amsterdam, 1984.

(40) Nishida, Y.; Kida, S. *Bull. Chem. Soc. Jpn.* **1972**, *45*, 461.

(41) Dyer, G.; Meek, D. W. *J. Am. Chem. Soc.* **1967**, *89*, 3983.

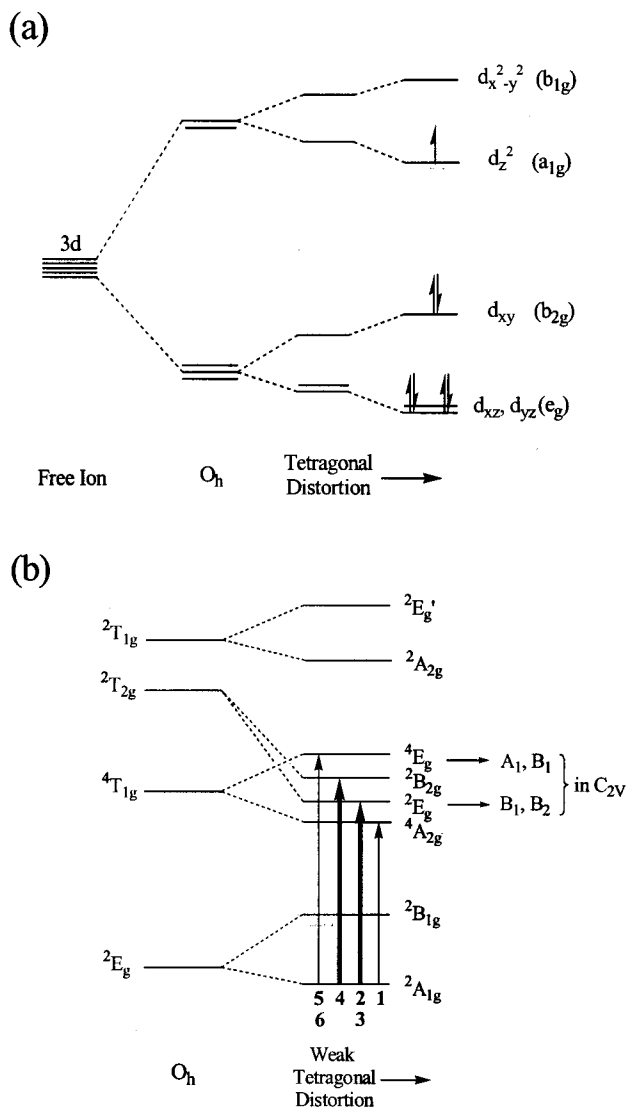


Figure 3. Illustration of the (a) d-orbital splitting diagram and (b) corresponding electronic term splittings for a low-spin d^7 system in tetragonal symmetry. Electronic transitions observed in Figure 2 are shown with light and dark arrows indicating their relative intensities.

quent ligand field distortion of the molecule toward C_{2v} local symmetry will lift the degeneracy of the E states thereby accounting for the six transitions in this energy region. Therefore, the absorption profile in Figure 2 derives from both spin-forbidden ${}^2A_{1g} \rightarrow {}^4A_{2g}$ (band 1) and ${}^2A_{1g} \rightarrow {}^4E_g$ transitions (bands 5 and 6) as well as spin-allowed ${}^2A_{1g} \rightarrow {}^2E_g$ (bands 2 and 3) and ${}^2A_{1g} \rightarrow {}^2B_{2g}$ excitations (band 4) involving $d_{xz,yz} \rightarrow d_z^2$ one-electron promotions (Figure 3b, Table 1). Transitions to the higher lying components of the ${}^2T_{1g}$ state are predicted⁴⁰ to occur at $\sim 22000 \text{ cm}^{-1}$, and indeed, a weak shoulder on a strong cyclam \rightarrow Ni(III) LMCT charge transfer transition ($\lambda_{\text{max}} = 370 \text{ nm}$)⁴² is observed at this energy. From these tentative spectral assignments, it is clear that the ligand field band centered at $\sim 13000 \text{ cm}^{-1}$ is diagnostic of the Ni(III) oxidation state.

Nickel Intermediates in the Oxidation of 1 by KHSO_5 . The reaction of **1** by KHSO_5 was examined in the presence and absence of the 17-base DNA hairpin loop in the presence of $0.1\text{--}1 \text{ M Cl}^-$. Mixing of **1** (100 mM phosphate, $\text{pH } 7.0$, 1

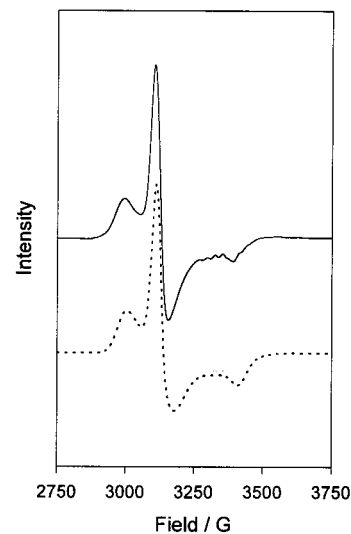


Figure 4. X-band EPR spectra (77 K) of the intermediates formed from the oxidation of **1** (3 mM) 30 s after reaction with 2.5 equiv of KHSO_5 in 100 mM phosphate buffer ($\text{pH } 7.0$) and 1 M Cl^- . The low-spin Ni(III) signal can be simulated with an axial species (65% , $g_{\perp} = 2.16$; $g_{\parallel} = 2.01$) and a rhombic component (35% , $g_x = 2.26$; $g_y = 2.20$, $g_z = 1.99$). A weak 7-line superhyperfine splitting is observed at $\sim 3300 \text{ G}$ indicative of two equivalent Cl^- ligands.

M Cl^-) and KHSO_5 (2.5 equiv) in the absence of DNA followed by freeze-quenching of the reaction with liquid N_2 (30 s) yielded the EPR spectrum shown in Figure 4 (solid line). The profile indicates formation of a low-spin $S = 1/2$ species which can be identified as a Ni(III) center. Spin quantitation of the signal indicates that approximately 11% of the nickel is in the Ni(III) form with the remainder in the EPR-silent Ni(II) state (vide infra). Close inspection of the feature at 3400 G reveals a 7-line superhyperfine splitting pattern (second derivative analysis: $1:2:3:4:3:2:1$) of the high-field component of the signal from two axial Cl^- ions. Spectral simulation shows that the signal is actually a $65\%:35\%$ mixture of an axial species with $g_{\perp} = 2.16$ and $g_{\parallel} = 2.01$, as well as a rhombic counterpart with $g_x = 2.26$, $g_y = 2.20$, and $g_z = 1.99$. The spectrum of the axial species is identical to that of the Ni(III) dichloride transient shown in Figure 1b in the presence of Cl^- . Similar results are obtained in the presence of the 17-base DNA substrate ($1:1 \text{ Ni:DNA}$; 1 mM) with the same buffer/salt concentrations. Importantly, under our experimental conditions, we do not observe a 3- or 5-line superhyperfine coupling pattern which would be expected if direct inner-sphere coordination by one or two nitrogen atoms from N7 of guanine were present in sufficient yield.^{34,35,37}

If the progress of the reaction is monitored over a period of 5 min (Figure 5), the Ni(III) EPR signal begins to diminish due to reduction of the Ni(III) species to Ni(II). Interestingly, the rhombic form decays to Ni(II) more rapidly than the axial species (Figure 5a). The same behavior is observed in the presence of the 17-base DNA substrate with only a small difference in the amount of the rhombic component present after 5 min (Figure 5b). The variations in the time scales for reduction may indicate that the two forms have disparate Ni(III/II) redox potentials. Since axial coordination by Cl^- ions is known to stabilize the Ni(III) form by reducing the Ni(III/II) redox potential,³⁷ the axial Ni(III) dichloride species can be detected at longer reaction times. In addition to the EPR signature of the Ni(III) species, the weak optical band near 770 nm can also be detected by rapid-scan UV-vis during the time course of the oxidation.

(42) Zeigerson, E.; Ginzburg, G.; Schwartz, N.; Luz, Z. *J. Chem. Soc., Chem. Commun.* **1979**, 241.

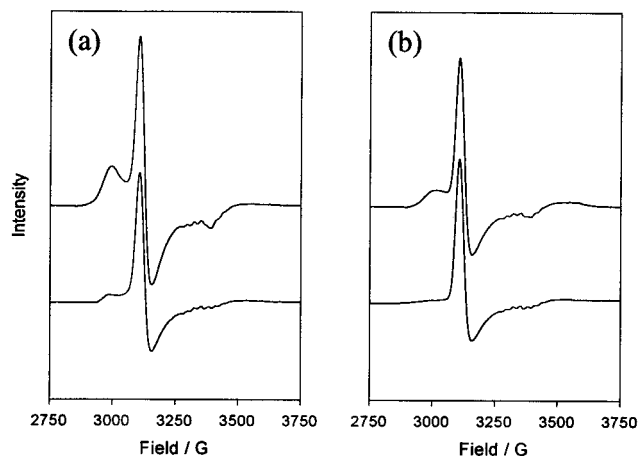


Figure 5. X-band EPR spectra (77 K) of the Ni(III) intermediates formed following reaction of **1** with 2.5 equiv of KHSO_5 in 100 mM phosphate buffer (pH 7.0) and 1 M Cl^- . Spectra are obtained 30 s (upper) and 5 min (lower) into the reaction in (a) the absence and (b) the presence of the 17-base DNA hairpin loop. The rhombic component of the low-spin Ni(III) signal decays rapidly to an EPR silent Ni(II) form leaving the axial Ni(III) dichloride species at longer times. The 7-line superhyperfine splitting of $g_{||}$ indicates that the axial species is stabilized by chloride coordination.

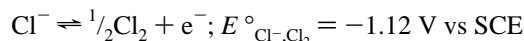
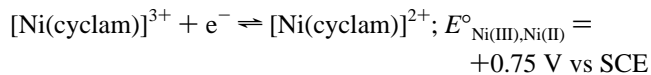
In general, the same spectral features and trends are observed in the EPR spectra as a function of $[\text{Cl}^-]$. The only differences involve the intensity of the Ni(III) signal detected. When $[\text{Cl}^-]$ is decreased to 400 mM and finally to 100 mM, spin quantitation of the EPR spectra at 30 s after initiation of the reaction indicates 15% and 70% of the Ni(III) species detected, respectively. This suggests that Cl^- is participating in some manner either by inhibiting the formation of the Ni(III) intermediate or by increasing the rate of reduction of the Ni(III) species to Ni(II) via an outer-sphere process. Interestingly, precedence exists for the formation of Cl_2 via oxidation of Cl^- by KHSO_5 (eqs 2 and 3).⁴³ Under our conditions, the formation of Cl_2 is readily



detected by GC-MS, confirming oxidation of Cl^- by KHSO_5 .⁴³ Reactions 2 and 3 are not surprising when one considers the highly positive potential for reduction of KHSO_5 (1.8 V vs SCE),⁴ and $\text{SO}_4^{\bullet-}$ (2.5 V vs SCE)⁴ formed by oxidation of Ni(II), and the modest potential required to oxidize Cl^- (1.12 V vs SCE).⁴⁴ Equations 2 and 3 partially explain the reduced amount of the Ni(III) intermediate detected at higher Cl^- concentrations as the oxidants HSO_5^- and $\text{SO}_4^{\bullet-}$ are effectively consumed by excess Cl^- . This reaction scheme is also in accordance with the reported inhibition in the DNA-modification activity for Ni(II) complex/ KHSO_5 reactions under high Cl^- concentrations.^{17,45} These conditions cause nucleobase oxidation in contrast to direct strand scission or formation of C4'-hydroxylated nucleotide lesions which are dominantly observed with Ni(II) peptide complexes under low salt conditions.^{16,17}

The decrease in the amount of Ni(III) detected by spin quantitation as $[\text{Cl}^-]$ is increased has a second origin. At Ni-

(III) concentrations of 3 mM and very high ionic strengths ($[\text{Cl}^-] > 400$ mM), rapid reduction of the Ni(III) center occurs via oxidation of Cl^- to yield $\text{Ni}(\text{cyclam})\text{Cl}_2$ as an orange precipitate. At 1 M Cl^- , $-\text{d}[\text{Ni(III)}]/\text{d}t$ is second order in $[\text{Ni(III)}]$ ($R^2 = 0.99$), which is consistent with previous reports of the oxidation of Br^- by Ni(III) complexes.⁴⁶ However, solely on the basis of redox potentials, the oxidation of Cl^- by $[\text{Ni}(\text{cyclam})]^{3+}$ is endergonic by -0.37 V:



This notwithstanding, at relatively high Cl^- concentrations, the precipitation of $\text{Ni}(\text{cyclam})\text{Cl}_2$ drives the oxidation of Cl^- by depleting the solution of $[\text{Ni}(\text{cyclam})]^{2+}$, thereby making the effective potential of the $[\text{Ni}(\text{cyclam})]^{3+}$ - $[\text{Ni}(\text{cyclam})]^{2+}$ couple more positive. One can modify the Nernst equation for the $[\text{Ni}(\text{cyclam})]^{3+}$ - $[\text{Ni}(\text{cyclam})]^{2+}$ couple by incorporating into it the solubility product (K_{sp}) for $\text{Ni}(\text{cyclam})\text{Cl}_2$:

$$E_{\text{Ni(III),Ni(II)}} = E^\circ_{\text{Ni(III),Ni(II)}} - 0.0592 \log \frac{K_{\text{sp}}}{[[\text{Ni}(\text{cyclam})]^{3+}][\text{Cl}^-]^2} \quad (4)$$

From eq 4, it is clear that the smaller the value of K_{sp} , the greater the shift of $E_{\text{Ni(III),Ni(II)}}$ to more positive potentials. If, for $[[\text{Ni}(\text{cyclam})]^{3+}] = 1.0$ mM and $[\text{Cl}^-] = 1$ M, we assume that $K_{\text{sp}} \leq 5.6 \times 10^{-10}$, the effective value of $E_{\text{Ni(III),Ni(II)}}$ becomes sufficiently positive that the oxidation of Cl^- by $[\text{Ni}(\text{cyclam})]^{3+}$ becomes thermodynamically favorable. This argument appears to be valid since K_{sp} for a six-coordinate, neutral Ni(II) macrocyclic species in water at pH 7.0 would be expected to be well below 5.6×10^{-10} . This is in accordance with published K_{sp} values which are on the order of 10^{-20} for neutral Ni(II) disulfides.⁴⁴

At lower $[\text{Cl}^-]$ (100, 400 mM), which are required to generate sufficient amounts of the Ni(III) intermediate to monitor over longer reaction times (1 h), the mixed axial/rhombic Ni(III) signal is once again detected immediately upon mixing (30 s) (Figure 6a). The rhombic component decays within 10 min, leaving the axial species with the diagnostic 7-line Cl^- superhyperfine coupling after 1 h (Figure 6b). It is clear from these results that the Ni(III) oxidation state, at least thermodynamically, prefers to bind Cl^- in the axial positions to other counterions present in solution or the 17-base DNA substrate.

In an effort to evaluate the ability of N7 of guanine to bind to the Ni(III) center via inner-sphere coordination, we have examined the EPR spectrum of a 1:1 ratio of **1**:DNA in the presence of 100 mM NaCl and 2.5 equiv of KHSO_5 (Figure 7). Promptly upon addition of KHSO_5 (15 s), the same axial Ni(III) species with $g_{\perp} = 2.16$ and $g_{||} = 2.01$ is observed in the presence of DNA. The 7-line superhyperfine splitting of $g_{||}$ at 2.01 (second derivative analysis: 1:2:3:4:3:2:1) indicates that, under these conditions, the predominant species in solution is the axial Ni(III) dichloride with no detectable presence of axial coordination to Ni(III) from the DNA substrate. Identical axial EPR spectra are obtained from a 1:1 ratio of **2**:DNA at $\text{Cl}^- > 100$ mM further supporting the preference of the Ni(III) center to bind to Cl^- rather than N7 of guanine. These results do not completely rule out the existence of the latter interaction but

(43) Dieter, R. K.; Nice, L. E.; Velu, S. E. *Tetrahedron Lett.* **1996**, 37, 2377.

(44) *CRC Handbook of Chemistry and Physics*, 73rd ed.; CRC Press: Boca Raton, 1992-1993.

(45) Tang, N.; Muller, J. G.; Burrows, C. J.; Rokita, S. E. *Biochemistry* **1999**, 38, 16648.

(46) Jaacobi, M.; Meyerstein, D.; Lilie, J. *Inorg. Chem.* **1979**, 18, 429.

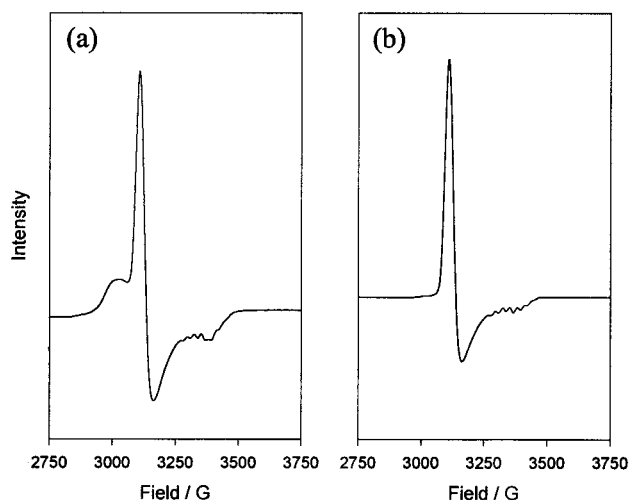


Figure 6. Frozen glass EPR spectra (77 K) of the oxidation of **1** (3 mM) by 2.5 equiv of KHSO_5 in 400 mM Cl^- (a) 30 s and (b) 1 h after initiation of the reaction. Both rhombic and axial species are present at early times while only the axial dichloride species persists after 1 h.

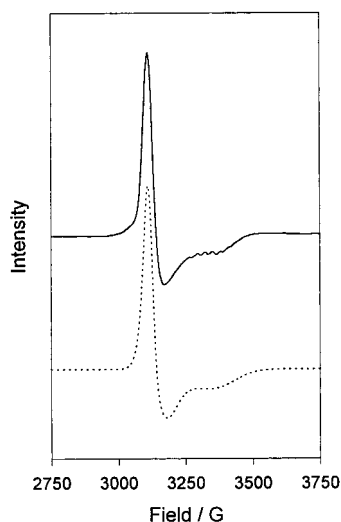


Figure 7. Observed (—) and calculated (···) X-band EPR spectra of the **1**/ KHSO_5 reaction (30 s) in 100 mM Cl^- at 77 K in the presence of the 17-base DNA hairpin loop. Even at reduced Cl^- concentrations, axial coordination is evident in the 7-line superhyperfine splitting pattern of $g_{||}$. Simulated EPR parameters: $g_{\perp} = 2.16$; $g_{||} = 2.01$.

rather indicate that under our conditions the solution population of guanine-ligated Ni(III), if present, is low.

The absence of inner-sphere coordination by N7 of guanine does not preclude binding of the 6-coordinate tetragonal Ni(III) dichloride complex to DNA. Figure 8 shows the visible region CD spectra of **2** and a 1:1 ratio of **2**:DNA (1 mM) under high salt conditions (1 M Cl^-) which ensures formation of the dichloride species in the presence of DNA. At these concentrations, CD bands from ligand field transitions are weak and not prominently observed. However, the considerably more intense cyclam \rightarrow Ni(III) LMCT transition centered at ~ 370 nm in the optical spectrum⁴² can be used as a suitable spectroscopic handle to evaluate the influence of the DNA substrate on the CD spectrum of the Ni(III) dichloride species derived from **2**. Tetraaza macrocycles have five possible configurations based on the stereochemistry of the donor nitrogen atoms. Coordinating solvents or pendant functional groups are known to induce changes in the population of these configurations.⁴⁷ Thus it is not surprising that $[\text{Ni}(\text{cyclam})\text{Cl}_2]^+$ exhibits a detectable CD

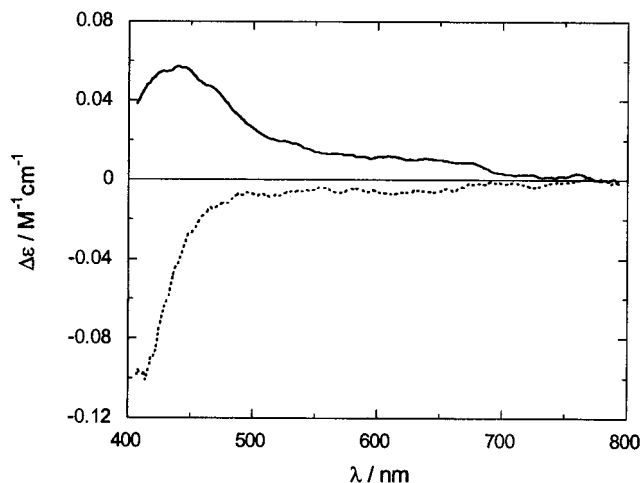


Figure 8. Visible region CD spectra of **2** (1 mM) at pH 7.0 and 1 M Cl^- in the absence (—) and presence (···) of the 17-base hairpin loop at 298 K. The spectra show inversion of the sign of the dichroism for absorption from the cyclam \rightarrow Ni(III) charge transfer transition near 400 nm indicative of metal complex–DNA binding.

signal. As shown in Figure 8, the presence of the 17-base oligonucleotide induces both an intensity increase and a sign inversion of the CD signal for the Ni(III) dichloride species present in the solution. Under these same solution conditions, no induced CD is observed for $[\text{Ni}(\text{cyclam})]^{2+}$ in the presence of DNA. These results are consistent with the demonstrations that $[\text{Ni}(\text{cyclam})]^{2+}$ does not bind to guanine monophosphate by NMR, nor convert poly(dG-dC) from B to Z helical form, while $[\text{Ni}(\text{cyclam})]^{3+}$ exhibits the opposite behavior.²⁵ Since Figure 7 shows that both axial positions are occupied by Cl^- under conditions as low as 100 mM Cl^- , such a conversion is likely occurring via outer-sphere binding of the charged $[\text{Ni}(\text{cyclam})\text{Cl}_2]^+$ complex and not through inner-sphere (N7) coordination to the metal under our experimental conditions. Indeed, there is general precedence for this type of outer-sphere binding and subsequent conversion of B to Z helical form by organic solvents⁴⁸ and polyamines,⁴⁹ as well as bimetallic $[\text{Pt}_2(\text{diamine})_4]^{4+}$ complexes⁵⁰ and Ru- and Fe(phen)₃²⁺.⁵¹ Moreover, NiCl_2 induces conversion of B to Z helical form in poly(dG-dC) but does not show Fermi contact induced paramagnetic NMR line shifting indicative of N7 coordination.⁴⁵ Cumulatively, these results indicate that, in the presence of a large excess of chloride ion, the Ni(III) center binds Cl^- in the axial positions very quickly to stabilize the high oxidation state thereby inhibiting inner-sphere binding by the neutral N7 of guanine to the Ni(III) center in high yield. This does not preclude interaction of $[\text{Ni}(\text{cyclam})\text{Cl}_2]^+$ with DNA. Rather, binding of the 6-coordinate complex to DNA is demonstrated by the inverted sign of the CD signal of the complex in the presence of the 17-base oligonucleotide.

During the oxidation of **1** by KHSO_5 , the starting orange solution turns first to the green color characteristic of the Ni(III) species and, subsequently, to a pale yellow color after approximately 30 min. At very short reaction time scales (< 2 s),

(47) Suh, M. P. *Macrocyclic Chemistry of Nickel*. In *Advances in Inorganic Chemistry*; Sykes, G., Ed.; Academic Press: Orlando, 1997; Vol. 44, p 93.

(48) Tomasz, M.; Barton, J. K.; Magliozzo, C. C.; Tucker, D.; Lafer, E. M.; Stollar, B. D. *Proc. Natl. Acad. Sci. U.S.A.* **1983**, *80*, 2874.

(49) Haworth, I. S.; Rodger, A.; Richards, W. G. *J. Biomol. Struct. Dyn.* **1992**, *10*, 195.

(50) Johnson, A.; Qu, Y.; Houten, B. V.; Farrell, N. *Nucleic Acids Res.* **1992**, *20*, 1697.

(51) Haerd, T.; Hiort, C.; Norden, B. *J. Biomol. Struct. Dyn.* **1987**, *5*, 89.

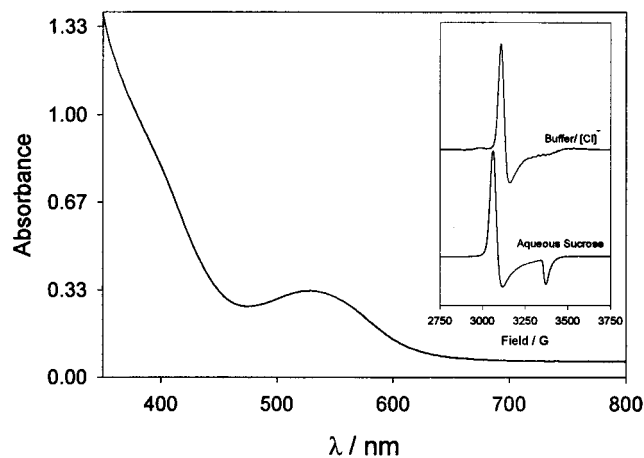


Figure 9. Electronic absorption spectrum of **1** (0.3 mM) following reaction with 1.25 equiv of KHSO_5 in water. X-band EPR spectra of this red species at 77 K are shown (inset) in both 100 mM phosphate buffer (pH 7.0) and 1 M Cl^- (upper; $g_{\perp} = 2.16$; $g_{\parallel} = 2.01$) and saturated aqueous sucrose solution (lower; $g_{\perp} = 2.20$; $g_{\parallel} = 2.02$). The low-spin signal and presence of the dichloride superhyperfine coupling identify this species as a Ni(III) dichloride center with a deprotonated cyclam ligand.

the solution briefly passes through a red intermediate that decays rapidly en route to the final yellow solution products. To date, the specific identity of the final solution products has not been reported due to their complexity, but in light of the high redox potentials for KHSO_5 and $\text{SO}_4^{\bullet-}$, these likely derive from Ni(II) products of the oxidized cyclam ligand.²⁹ Our observed reduction of Ni(III) to Ni(II) in the EPR and the pronounced changes in the optical spectrum of the starting $[\text{Ni}(\text{cyclam})]^{2+}$ ($\lambda_{\text{max}} = 450$ nm) are consistent with the formation of the oxidized cyclam products. In an effort to identify the intermediates in the time course of the reaction, we have successfully trapped the red species both in water and in the presence/absence of DNA solutions using only 1.25 equiv of KHSO_5 (Figure 9). Under these conditions, the intermediate lives for several hours in solution at room temperature. The electronic absorption spectrum of this species shows a prominent absorption band at 530 nm with stronger features at 400 nm and to higher energy. The EPR spectra of the red intermediate both in water and in buffered solution (pH 7.0) conditions (Figure 9, inset) once again reveal an axial Ni(III) species with two chlorides bound in the apical positions in the presence of excess chloride. Spin quantitation indicates that, under these reaction conditions, approximately 50% of the nickel present in solution is in the Ni(III) form. Subsequent addition of 1.25 equiv of KHSO_5 consumes the red intermediate and drives the reaction toward completion. In contrast, addition of chloride to the red species has no effect on the stability of the intermediate.

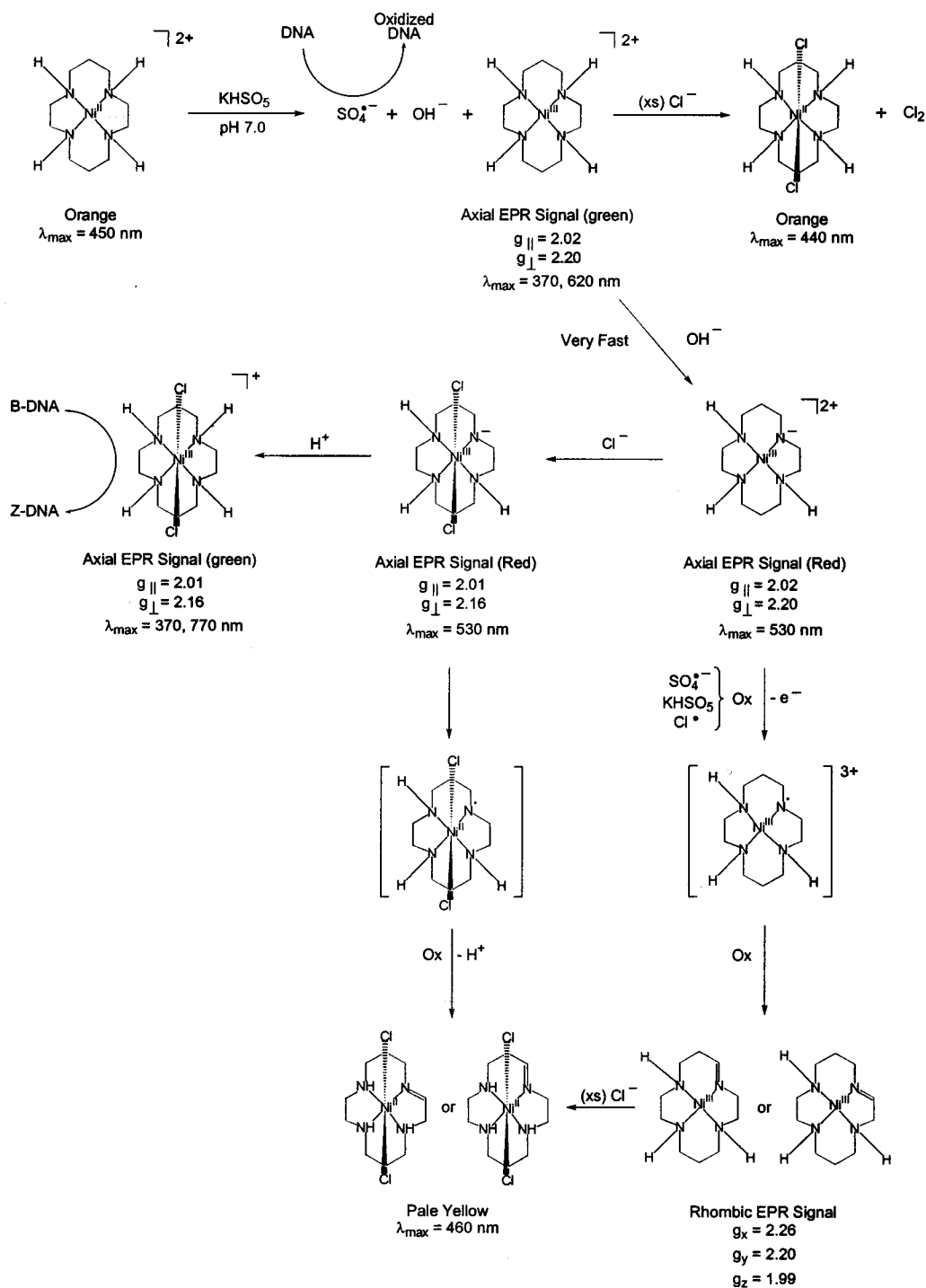
The band at 530 nm in the electronic absorption spectrum is a signature of the identity of the red Ni(III) intermediate. Fabrizio et al. have shown via pH titration that the cyclam ligand can be deprotonated in the Ni(III) bound form at pH 7.0 to yield a red Ni(III) complex with λ_{max} at 539 nm.⁵² Therefore, it is clear that during the oxidation of **1** by KHSO_5 , deprotonation of the cyclam ligand⁵³ is occurring presumably due to the decrease in the pK_a of the amine protons by formation of the Ni^{3+} oxidation state and the presence of OH^- formed during the decomposition of KHSO_5 at the nickel center.

Implications to the Mechanism of DNA Modification by KHSO_5 . Scheme 2 illustrates the cumulative results of these studies and their relevance to the mechanism of DNA modification by the reaction of **1** with KHSO_5 . Reaction of **1** in the

diaquo form at pH 7.0 generates a transient Ni(III) species ($g_{\perp} = 2.20$ and $g_{\parallel} = 2.02$; $\lambda_{\text{max}} = 370, 620$ nm) along with the reported concomitant formation of $\text{SO}_4^{\bullet-}$ and OH^- . The time scales of the freeze/quench EPR studies presented above do not permit determination of whether $\text{SO}_4^{\bullet-}$ is created via an inner- or outer-sphere reaction pathway. Since detection of the Ni(III) species under low Cl^- conditions (100 mM) can be made in 70% yield, it is clear that this oxidation state is the predominant metastable form. Four additional transient Ni(III) structures are subsequently produced from this original Ni(III) species. The initial species formed is a red intermediate ($g_{\perp} = 2.20$ and $g_{\parallel} = 2.02$; $\lambda_{\text{max}} = 530$ nm) generated by deprotonation of the cyclam ligand, likely by OH^- formed in the oxidation reaction. This species can subsequently acquire two axial chloride ligands to form the red dichloride analogue ($g_{\perp} = 2.16$ and $g_{\parallel} = 2.01$; $\lambda_{\text{max}} = 370$ nm) which has electronic properties very similar to those of the Ni(III) precursor, but is distinguished by 7-line superhyperfine coupling to the axial Cl^- ligands.

The red deprotonated intermediates are unstable in excess KHSO_5 and decay rapidly, each by either of two pathways. First, the red dichloride intermediate can be reprotonated by the buffered solution (pH 7.0) to yield the metastable $[\text{Ni}(\text{cyclam})\text{Cl}_2]^+$ species ($g_{\perp} = 2.16$ and $g_{\parallel} = 2.01$; $\lambda_{\text{max}} = 370, 770$ nm) observed in the EPR studies at reaction times > 1 min. This green species has been shown to convert DNA from B to Z helical form and, under our conditions, inverts the sign of the Ni(III) CD signal. Second, the Ni(III) center can oxidize the cyclam ligand to form a transient Ni(II)–ligand radical species which is subsequently oxidized to form unsaturated ligand products of Ni(II)cyclam ($\lambda_{\text{max}} = 460$ nm). The latter mechanistic step has been proposed to account for the slow degradation of trivalent nickel compounds with secondary nitrogen donors.^{52,54} Third, the red Ni(III) precursor can be oxidized rapidly, possibly by $\text{SO}_4^{\bullet-}$, to form a rhombic species ($g_x = 2.26$, $g_y = 2.20$, and $g_z = 1.99$) that derives from a Ni(III) center without axial Cl^- ligation. The specific origin of the rhombic transient cannot be unequivocally identified based on the EPR data. However, rhombicity in the EPR signal can most readily be achieved by chemical modification of the cyclam macrocycle which removes the local symmetry of the x and y axes. Although chemical inequivalency is not a prerequisite for rhombic symmetry,^{55–57} a very high percentage of Ni(III) complexes exhibit axial spectra.^{33,35,37,58} Therefore, oxidation of the cyclam ring and imine formation would likely give rise to a transient Ni(III) center with rhombic symmetry. Since the ligand is susceptible to deprotonation (Figure 9) and a proposed mechanism for Ni(III) reduction to Ni(II) involves ligand oxidation resulting in yellow Ni(II) products, these suggest that the identity of the rhombic species may be a Ni(III) complex of an unsaturated cyclam ligand. The Ni(II) form of this complex is yellow with $\lambda_{\text{max}} = 460$ nm⁵² and could easily be formed from oxidation of Cl^- as observed for $[\text{Ni}(\text{cyclam})]^{3+}$ (vide supra). Unsaturated Ni(III) complexes are known to have considerably higher reduction potentials (> 0.3 V)²³ than their saturated

- (52) De Santis, G.; Fabbrizzi, L.; Poggi, A.; Taglietti, A. *Inorg. Chem.* **1994**, *33*, 134.
 (53) Bal, W.; Djuran, M. I.; Margerum, D. W.; Gray, E. T., Jr.; Mazid, M. A.; Tom, R. T.; Nieboer, E.; Sadler, P. J. *J. Chem. Soc., Chem. Commun.* **1994**, 1889.
 (54) Zilbermann, I.; Golab, G.; Cohen, H.; Meyerstein, D. *J. Chem. Soc., Dalton Trans.* **1997**, 141.
 (55) Holm, R. H.; Maki, A. H.; Edelstein, N.; Davison, A. *J. Am. Chem. Soc.* **1964**, *86*, 4580.
 (56) Bhattacharya, S.; Mukherjee, R.; Chakravorty, A. *Inorg. Chem.* **1986**, *25*, 3448.
 (57) Drago, R. S.; Baucom, E. I. *Inorg. Chem.* **1972**, *11*, 2064.
 (58) Fairbank, M. G.; McAuley, A. *Inorg. Chem.* **1986**, *25*, 1233.

Scheme 2. Proposed Mechanism for the Oxidation of $[\text{Ni}(\text{cyclam})]^{2+}$ by KHSO_5 and Its Relation to DNA Modification

counterparts, making this reaction thermodynamically feasible. It is also possible that the complex degrades to a further unsaturated form, by deprotonation and subsequent oxidation of the ligand by the Ni(III) center.^{52,54}

One of the key results of this work is that, under our conditions, the $[\text{Ni}(\text{cyclam})]^{3+}$ species in the presence of excess Cl^- does not exhibit inner-sphere coordination to DNA to a measurable extent, implying that a $\text{N7-Ni(III)-SO}_4^{*-}$ species is not likely to form in significant yield during the DNA modification pathway. From chemical potential and electrochemical perspectives, binding of anionic chloride ligands will rapidly stabilize the Ni(III) center. Indeed, this is born out by experiment as the redox potential for $[\text{Ni}(\text{cyclam})\text{Cl}_2]^+$ is 0.25

V more negative than that for $[\text{Ni}(\text{cyclam})]^{3+}$.³⁷ To this end, a mechanism involving rapid formation of $[\text{Ni}(\text{cyclam})\text{Cl}_2]^+$ and consequently free SO_4^{*-} would relieve the necessity for the highly reactive Ni(III)-SO_4^{*-} intermediate to diffuse in solution to the DNA substrate prior to guanine oxidation.

These observations shed light on the primary intermediates and mechanism responsible for DNA modification by the reaction of $[\text{Ni}(\text{cyclam})]^{2+}$ with KHSO_5 . Burrows et al. have shown that the efficiency for DNA oxidation correlates with the in-plane donor strength of the macrocycle ligand field such that a stable square planar complex with high Ni(III)/Ni(II) redox couple is obtained.^{15,23} The open coordination positions could then bind oxidant or DNA transiently. The requirement for labile

axial ligands defines $[\text{Ni}(\text{cyclam})]^{2+}$ as a poor DNA oxidation catalyst as it exists as a mixture of 4- and 6-coordinate structures (counterion or aquo coordination) in solution and consequently, yields only 6% modified DNA.^{15,23} Indeed, the inability of $[\text{Ni}(\text{cyclam})]^{2+}$ to bind to DNA (inner or outer sphere) and convert B to Z helical form has been verified by NMR and CD spectroscopies, respectively, in the absence of Cl^- .¹⁹ Interestingly, the same experimental results are also obtained for the more rigorously square planar complex $[\text{NiCR}]^{2+}$,¹⁹ which is a much better DNA modification agent (46%).²³ This implies that DNA modification by $[\text{NiCR}]^{2+}$ may not require inner-sphere N7 coordination by the Ni(II) forms in order to induce DNA modification upon reaction with KHSO_5 . As a caveat, certain Ni(II) complexes do indeed show N7 inner-sphere coordination above a background of nonspecific association,²⁶ but importantly in the context of the present work, these results are obtained in the absence of chloride counterion, which, as the present study demonstrates, may influence the availability of axial positions for N7 coordination.

Unfortunately, far less data is available for the binding of Ni(III) complexes to DNA. To date, only $[\text{Ni}(\text{cyclam})]^{3+}$ has been systematically investigated using NMR and CD techniques.¹⁹ In contrast to $[\text{Ni}(\text{cyclam})]^{2+}$, in the absence of Cl^- the Ni(III) complex does exhibit binding to DNA, likely through the axial positions, in addition to promoting the B to Z DNA conversion. Since our results show that, in the presence of Cl^- and DNA, the Ni(III) centers detected are coordinatively saturated by axial chlorides, binding of the complex to DNA under these conditions (Figure 8) can only be explained either by an outer-sphere event or by an equilibrium where a small percentage of the Ni(III) complex is participating in the binding step. It is clear from the EPR data that, in the presence of Cl^- , the N7–Ni(III) species is not the primary form present in solution.

Since other nickel compounds such as $[\text{NiCR}]^{2+}$ have considerable DNA oxidation efficiencies yet do not bind DNA in the Ni(II) form,¹⁹ and coordinatively saturated $[\text{Ni}(\text{cyclam})\text{Cl}_2]^+$ can potentially bind to DNA via an outer-sphere pathway, it is possible, although not yet documented experimentally, that DNA modification by these nickel compounds in the presence of excess Cl^- does not require axial ligation to the metal in either oxidation state. Within this proposed scheme for $[\text{Ni}(\text{cyclam})]^{2+}$, oxidation to Ni(III) by KHSO_5 may generate freely diffusing $\text{SO}_4^{\bullet-}$ which reacts rapidly in solution with either the cyclam ligand, Cl^- , or a guanine base. This provides an alternative explanation for the inability to detect free $\text{SO}_4^{\bullet-}$ radicals in solution for the reaction of $[\text{NiCR}]^{2+}$ with KHSO_5 .¹⁸ Here, radical quenching by the macrocyclic ligand would effectively reduce the diffusion length of the intermediate and hence the amount of free $\text{SO}_4^{\bullet-}$ in solution. This proposal is consistent with the reduced DNA oxidation activity of $[\text{NiCR}]^{2+}$ (~48%) vs CoCl_2 under identical conditions.²² Moreover, the correlation of guanine oxidation patterns generated by the $\text{CoCl}_2/\text{KHSO}_5$ reaction^{18,59} with total heterocycle exposure of guanine rather than N7 exposure specifically, coupled with detection of

freely diffusing $\text{SO}_4^{\bullet-}$, suggests that the presence or absence of the organic macrocycle can greatly influence the detectable reaction intermediates and DNA oxidation results.

The fact that the coordinatively saturated $[\text{Ni}(\text{cyclam})\text{Cl}_2]^+$ shows a strong interaction with DNA in the CD spectrum, coupled with the absence of N7 superhyperfine coupling to Ni(III) both during the oxidation reaction and in 1:1 2:DNA experiments in the presence of Cl^- , supports the conclusion that the N7–Ni(III)– $\text{SO}_4^{\bullet-}$ transient is not a major intermediate under our conditions. If this species were formed in significant yield, immediately following release of $\text{SO}_4^{\bullet-}$, the Ni(III) center would likely remain coordinated to N7 of the anionic biopolymer. Thus the Ni(III) EPR signal would exhibit detectable superhyperfine signals from axial nitrogen, unless this species is produced in yields too low to detect. Since $[\text{Ni}(\text{cyclam})]^{2+}$ has been shown not to bind to DNA prior to oxidation,¹⁹ the probability that Ni(III)– $\text{SO}_4^{\bullet-}$ is capable of diffusing intact to the DNA target to form the N7–Ni(III)– $\text{SO}_4^{\bullet-}$ intermediate is low. The EPR results presented above support this conclusion but do not exclusively rule out formation of N7–Ni(III)– $\text{SO}_4^{\bullet-}$ in concentrations too low to detect.

Conclusion

We have demonstrated that, upon oxidation of **1** by KHSO_5 , several transient Ni(III) species are produced that derive from varying axial ligation and modification of the cyclam ring. The rhombic form decays rapidly in solution while the axial form is stabilized via apical coordination by two Cl^- ligands. This is the dominant species in solution under excess salt conditions. Similar results are obtained in the presence of the 17-base DNA hairpin loop, suggesting that inner-sphere coordination to the Ni(III) intermediate by DNA is not occurring in significant concentration under our conditions. The absence of metal coordination by N7 of guanine does not preclude binding of the 6-coordinate Ni(III) complex to DNA. Rather, under our conditions, the complex appears to bind via an outer-sphere interaction. These results, coupled with the fact that $[\text{Ni}(\text{cyclam})]^{2+}$ does not bind to DNA in significant yield, imply that formation of a nickel–N7 species is not favored in either oxidation state and consequently the N7–Ni(III)– $\text{SO}_4^{\bullet-}$ is not the major intermediate under our conditions. Observation of ligand-deprotonated Ni(III) species and formation of yellow Ni(II) products suggest that ligand oxidation may be occurring following formation of $\text{SO}_4^{\bullet-}$ at the Ni(II) center. Under this assumption, the rhombic Ni(III) intermediate may result from this oxidized product. This implies that $\text{SO}_4^{\bullet-}$ may have a diminished lifetime in solution due to reaction with the cyclam ligand. Finally, our results contribute to and complement the detailed understanding of DNA modification by the reaction of Ni(II) complexes with KHSO_5 developed by reports of other research groups.

Acknowledgment. We are grateful to Professors Cynthia Burrows and Dennis Peters for helpful discussions as well as Mr. Lee Klein for technical assistance. The generous support of Indiana University is gratefully acknowledged.

(59) McLachlan, G. A.; Muller, J. G.; Rokita, S. E.; Burrows, C. J. *Inorg. Chim. Acta* **1996**, *251*, 193.